ceramics

MDPI

Article

On the Synthesis and Characterization of Lanthanide Metal-Organic Frameworks

Andrius Laurikenas, Aldona Beganskiene and Aivaras Kareiva *

Department of Inorganic Chemistry, Institute of Chemistry, Vilnius University, Naugarduko 24, LT-03225 Vilnius, Lithuania; andrius.lauriken@gmail.com (A.L.); aldona.beganskiene@chf.vu.lt (A.B.)
* Correspondence: aivaras.kareiva@chgf.vu.lt

Received: 28 March 2018; Accepted: 11 June 2018; Published: 12 June 2018

Abstract: In this study, lanthanide metal-organic frameworks $Ln(BTC)(DMF)_2(H_2O)$ (LnMOFs) are synthesized using the metal nitrates as lanthanide (Ln = La, Ce, Pr, Nd, Sm, Eu, Tb, Dy, Ho, Er, Tm, Yb and Lu) source and 1,3,5-benzenetricarboxylic acid (BTC) as a coordination ligand. X-ray diffraction (XRD) analysis, Fourier-transform infrared spectroscopy (FTIR), thermogravimetric (TG/DTG) analysis fluorescence spectroscopy (FLS), and scanning electron microscopy (SEM) are employed to characterize the newly synthesized LnMOFs.

Keywords: lanthanides; metal-organic framework; 1,3,5-benzentricarboxylic acid; synthesis; luminescence

1. Introduction

Metal-organic frameworks (MOFs), having zeolite-like network structure, are synthesized by self-assembly of polydentatic organic ligands and metal ions [1,2]. MOFs are characterized as materials having large surface area, highly porous structures, and large (tunable) pore volume. In today's world, MOF are used in aspects of gas storage, gas and liquid adsorption and separation, luminescence, catalysis, and in electrochemical biosensors for ultrasensitive detection [1–5].

The metal ion center has a key role for metal-organic frameworks. Lanthanides possess a unique electronic shell structure because their 4f electron shells are not completely filled, and the number of electrons in 4f shells varies, in this case, lanthanides have relatively high coordination numbers, which allows us to synthesize MOF with desired structures. The synthesis of lanthanide metal-organic framework is dependent on a variety of internal and external parameters, such as ionic radius, reaction temperature, atmosphere, coordinating solvents, and the nature of counter anions. Lanthanide metal-organic frameworks having high porosity, specific pore size, and 2D and 3D coordination networks could be used as heterogeneous catalysts in organic synthesis and solvent-free reactions [3,4,6,7]. General metal-organic framework synthesis types include solvothermal, hydrothermal, and solvent-free methods [8–11]. In this study, the solvothermal synthesis method was chosen, aiming for good crystallinity of synthesised MOFs [3,4].

In this work, the lanthanide metal-organic frameworks (LnMOFs) $Ln(BTC)(DMF)_2(H_2O)$ (Ln = La, Ce, Pr, Nd, Sm, Eu, Tb, Dy, Ho, Er, Tm, Yb and Lu) were synthesized using the solvothermal method [1–4] at elevated temperature. The lanthanide nitrates and 1,3,5-benzenetricarboxylic acid (BTC) were used as a metal ion center and ligand, respectively.

2. Experimental

Lanthanide nitrates, 1,3,5-benzentricarboxylic acid (BTC), *N*,*N*-dimethylformamide, and methanol were purchased from Aldrich and used directly without further purification. The syntheses of MOFs were performed using the following procedures:

La^{3+}(BTC)$(DMF)_2(H_2O)$ (LaMOF). $La(NO_3)_3{\cdot}6H_2O$ (0.322 g, 0.75 mmol) was dissolved in *N*,*N*-dimethylformide/water (3:1 *v*/*v*) mixture (20 mL). (0.116 g, 0.55 mmol) BTC was added and mixture was stirred for 30 min at room temperature. After complete dissolution the mixture was kept in the furnace at 65 °C for 24 h. The formed transparent rod-like crystals were filtered on a dense paper filter, washed with methanol (15) mL three times. Crystals were punt into chloroform for solvent exchange (removal of DMF) for 24 h, afterwards dried in air, which resulted in 0.195 g LaMOF, yield 45%.

The preparation procedures for other lanthanide MOFs were analogous for LaMOF and were performed using different starting materials.

Ce^{3+}(BTC)$(DMF)_2(H_2O)$ (CeMOF). Using $Ce(NO_3)_3{\cdot}6H_2O$ (0.324g, 0.75 mmol) and (0.116 g, 0.55 mmol) BTC. The synthesis yielded 0.231 g (51%) transparent rod-like $Ce^{3+}(BTC)(DMF)_2(H_2O)$ crystals.

Pr^{3+}(BTC)$(DMF)_2(H_2O)$ (PrMOF). Using $Pr(NO_3)_3{\cdot}6H_2O$ (0.324 g, 0.75 mmol) and (0.116 g, 0.55 mmol) BTC. The synthesis yielded 0.177 g (40%) green transparent rod-like $Pr^{3+}(BTC)(DMF)_2(H_2O)$ crystals.

Nd^{3+}(BTC)$(DMF)_2(H_2O)$ (NdMOF). Using $Nd(NO_3)_3{\cdot}6H_2O$ (0.326 g, 0.75 mmol) and (0.116 g, 0.55 mmol) BTC. The synthesis yielded 0.256 g (51%) slightly purple $Nd^{3+}(BTC)(DMF)_2(H_2O)$ powder.

Sm^{3+}(BTC)$(DMF)_2(H_2O)$ (SmMOF). Using $Sm(NO_3)_3{\cdot}4H_2O$ (0.331 g, 0.75 mmol) and (0.116 g, 0.55 mmol) BTC. The synthesis yielded 0.21 g (43%) yellowish rod-like $Sm^{3+}(BTC)(DMF)_2(H_2O)$ crystals.

Eu^{3+}(BTC)$(DMF)_2(H_2O)$ (EuMOF). Using $Eu(NO_3)_3{\cdot}5H_2O$ (0.332 g, 0.75 mmol) and (0.116 g, 0.55 mmol) BTC. The synthesis yielded 0.271 g (56%) white rod-like $Eu^{3+}(BTC)(DMF)_2(H_2O)$ crystals.

Gd^{3+}(BTC)$(DMF)_2(H_2O)$ (GdMOF). Using $Gd(NO_3)_3{\cdot}6H_2O$ (0.336 g, 0.75 mmol) and (0.116 g, 0.55 mmol) BTC. The synthesis yielded 0.203 g (52%) white $Gd^{3+}(BTC)(DMF)_2(H_2O)$ powder.

Tb^{3+}(BTC)$(DMF)_2(H_2O)$ (TbMOF). Using $Tb(NO_3)_3{\cdot}5H_2O$ (0.337 g, 0.75 mmol) and (0.116 g, 0.55 mmol) BTC. The synthesis yielded 0.271 g (56%) colourless rod-like $Tb^{3+}(BTC)(DMF)_2(H_2O)$ crystals.

Dy^{3+}(BTC)$(DMF)_2(H_2O)$ (DyMOF). Using $Dy(NO_3)_3{\cdot}6H_2O$ (0.340 g, 0.75 mmol) and (0.116 g, 0.55 mmol) BTC. The synthesis yielded 0.211 g (59%) yellowish rod-like $Dy^{3+}(BTC)(DMF)_2(H_2O)$ crystals.

Ho^{3+}(BTC)$(DMF)_2(H_2O)$ (HoMOF). Using $Ho(NO_3)_3{\cdot}5H_2O$ (0.342 g, 0.75 mmol) and (0.116 g, 0.55 mmol) BTC. The synthesis yielded 0.251 g (49%) pink rod-like $Ho^{3+}(BTC)(DMF)_2(H_2O)$ crystals.

Er^{3+}(BTC)$(DMF)_2(H_2O)$ (ErMOF). Using $Er(NO_3)_3{\cdot}6H_2O$ (0.343 g, 0.75 mmol) and (0.116 g, 0.55 mmol) BTC. The synthesis yielded 0.209 g (50%) pink rod-like $Er^{3+}(BTC)(DMF)_2(H_2O)$ crystals.

Tm^{3+}(BTC)$(DMF)_2(H_2O)$ (TmMOF). Using $Tm(NO_3)_3{\cdot}5H_2O$ (0.345 g, 0.75 mmol) and (0.116 g, 0.55 mmol) BTC. The synthesis yielded 0.148 g (36%) slightly green rod-like $Tm^{3+}(BTC)(DMF)_2(H_2O)$ crystals.

Yb^{3+}(BTC)$(DMF)_2(H_2O)$ (YbMOF). Using $Yb(NO_3)_3{\cdot}6H_2O$ (0.348 g, 0.75 mmol) and (0.116 g, 0.55 mmol) BTC. The synthesis yielded 0.199 g (41%) slightly green rod-like $Yb^{3+}(BTC)(DMF)_2(H_2O)$ crystals.

Lu^{3+}(BTC)$(DMF)_2(H_2O)$ (LuMOF). Using $Lu(NO_3)_3{\cdot}6H_2O$ (0.349 g, 0.75 mmol) and (0.116 g, 0.55 mmol) BTC. The synthesis yielded 0.192 g (45%) slightly green rod-like $Lu^{3+}(BTC)(DMF)_2(H_2O)$ crystals.

XRD data were collected at room temperature on a Rigaku Miniflex II system with a graphite monochromator, using Cu Kα1 radiation (speed 1°/min). FTIR analysis of compounds was conducted using a Bruker Alpha FTIR spectrometer with Platinum ATR single reflection diamond module. Thermal analyses were conducted from room temperature to 600 °C under air atmosphere using Perkin Elmer Pyris 1 TGA thermal analyser and Pyris software. The heating rate was 5 °C/min. Excitation and emission measurements were acquired using Edinburgh Instruments FLS980 fluorescence spectrometer.

The emission spectra were conducted in the solid state. Scanning electron microscope (SEM) Hitachi TM3000 was used to study the main morphological features of obtained crystals.

3. Results and Discussion

3.1. XRD Analysis

The synthesised fourteen lanthanide metal-organic frameworks were found to be isomorphous having very similar structures. However, only the structure of LaMOF is described here in detail (Figure 1).

LaMOF is a three-dimensional open framework. Each asymmetric unit contains one eight-coordinated La^{3+} ion, one BTC ligand, two coordinated DMF molecules, with eight oxygen atoms from four BTC ligands through two chelating carboxylate groups (O1–O4), two carboxylate groups (O5 and O6), and two terminal DMF molecules (O7 and O8). In the LaMOF molecule, one La^{3+} ion is linked with four phenyl groups through two chelating bidentate carboxylate groups and two monodentate carboxylate groups.

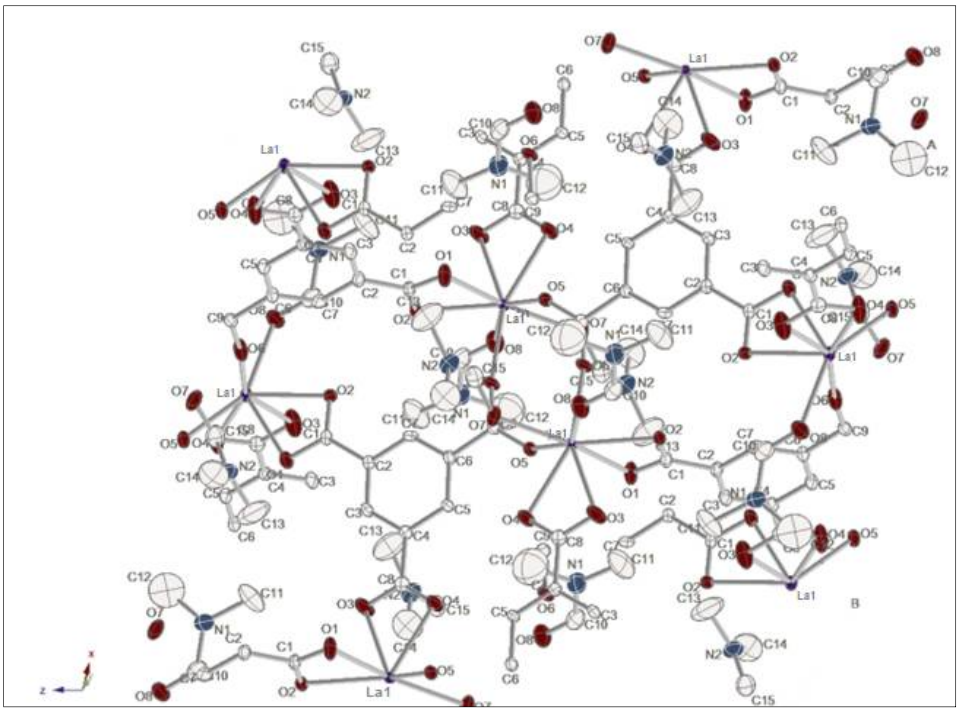

Figure 1. Coordination environment of $La(BTC)(DMF)_2(H_2O)$ (LaMOF) with atoms represented by thermal ellipsoids (40% probability level). The hydrogen atoms are omitted.

The XRD patterns LnMOFs are presented in Figure 2. As seen, the XRD patterns of $Ln(BTC)(DMF)_2(H_2O)$ (Ln = La, Ce, Eu, Gd, Tb, Dy, Ho, Tm, Yb and Lu) show good agreement with standard ICDD PDF patterns. The comparison of experimental and standard data demonstrates the formation of monophasic compounds under the applied synthesis conditions. Moreover, these MOFs were prepared with very well-developed crystalline structure. The XRD patterns of $Ln(BTC)(DMF)_2(H_2O)$ (Ln = Er, Pr, Nd and Sm) displayed lower crystallinity of synthesized compounds. (Figure 2) The crystallographic data of fabricated LnMOFs are summarized in Table 1.

Table 1. Crystallographic data of LnMOFs.

	LaMOF	**CeMOF**	**PrMOF**	**NdMOF**	**SmMOF**	**EuMOF**	**GdMOF**
Empirical Formula	$C_{15}H_{19}N_2O_9La$	$C_{15}H_{19}N_2O_9Ce$	$C_{15}H_{19}N_2O_9Pr$	$C_{15}H_{19}N_2O_9Nd$	$C_{15}H_{19}N_2O_9Sm$	$C_{15}H_{19}N_2O_9Eu$	$C_{15}H_{19}N_2O_9Gd$
Formula Weight	509.9	511.12	511.91	515.24	521.36	522.96	528.25
Crystal System	*monoclinic*	*monoclinic*	*monoclinic*	*monoclinic*	*monoclinic*	*monoclinic*	*monoclinic*
Space Group	*C*2/*c*	*C*2/*c*	*C*2/*c*	*C*2/*c*	*C*2/*c*	*C*2/*c*	*C*2/*c*
a (Å)	18.896	18.847	18.798	18.749	18.7	18.651	18.602
b (Å)	11.649	11.682	11.673	11.601	11.615	11.66	11.59
c (Å)	19.866	19.906	19.851	19.897	19.849	19.795	19.688
β (deg)	*75.447*	*72.783*	*73.13*	*74.4*	*72.97*	*73.11*	*72.9*
V ($Å^3$)	4232.6	4186.34	4168.43	4129.64	4122.17	4119.14	4057.03
Z	8	8	8	8	8	8	8
	TbMOF	**DyMOF**	**HoMOF**	**ErMOF**	**TmMOF**	**YbMOF**	**LuMOF**
Empirical Formula	$C_{15}H_{19}N_2O_9Tb$	$C_{15}H_{19}N_2O_9Dy$	$C_{15}H_{19}N_2O_9Ho$	$C_{15}H_{19}N_2O_9Er$	$C_{15}H_{19}N_2O_9Tm$	$C_{15}H_{19}N_2O_9Yb$	$C_{15}H_{19}N_2O_9Lu$
Formula Weight	530.24	533.82	536.25	538.58	540.25	544.36	545.96
Crystal System	*monoclinic*	*monoclinic*	*monoclinic*	*monoclinic*	*monoclinic*	*monoclinic*	*monoclinic*
Space Group	*C*2/*c*	*C*2/*c*	*C*2/*c*	*C*2/*c*	*C*2/*c*	*C*2/*c*	*C*2/*c*
a (Å)	18.568	18.493	18.44	18.401	18.382	18.299	18.258
b (Å)	11.63	11.58	11.647	11.649	11.592	11.592	11.578
c (Å)	19.741	19.51	19.698	19.68	19.632	19.557	19.592
β (deg)	*72. 97*	*72.79*	*72.945*	*73.03*	*72.92*	*72.98*	*72.58*
V ($Å^3$)	4072.3	3991	4044.5	4034.8	3998.8	3966.9	3951.62
Z	8	8	8	8	8	8	8

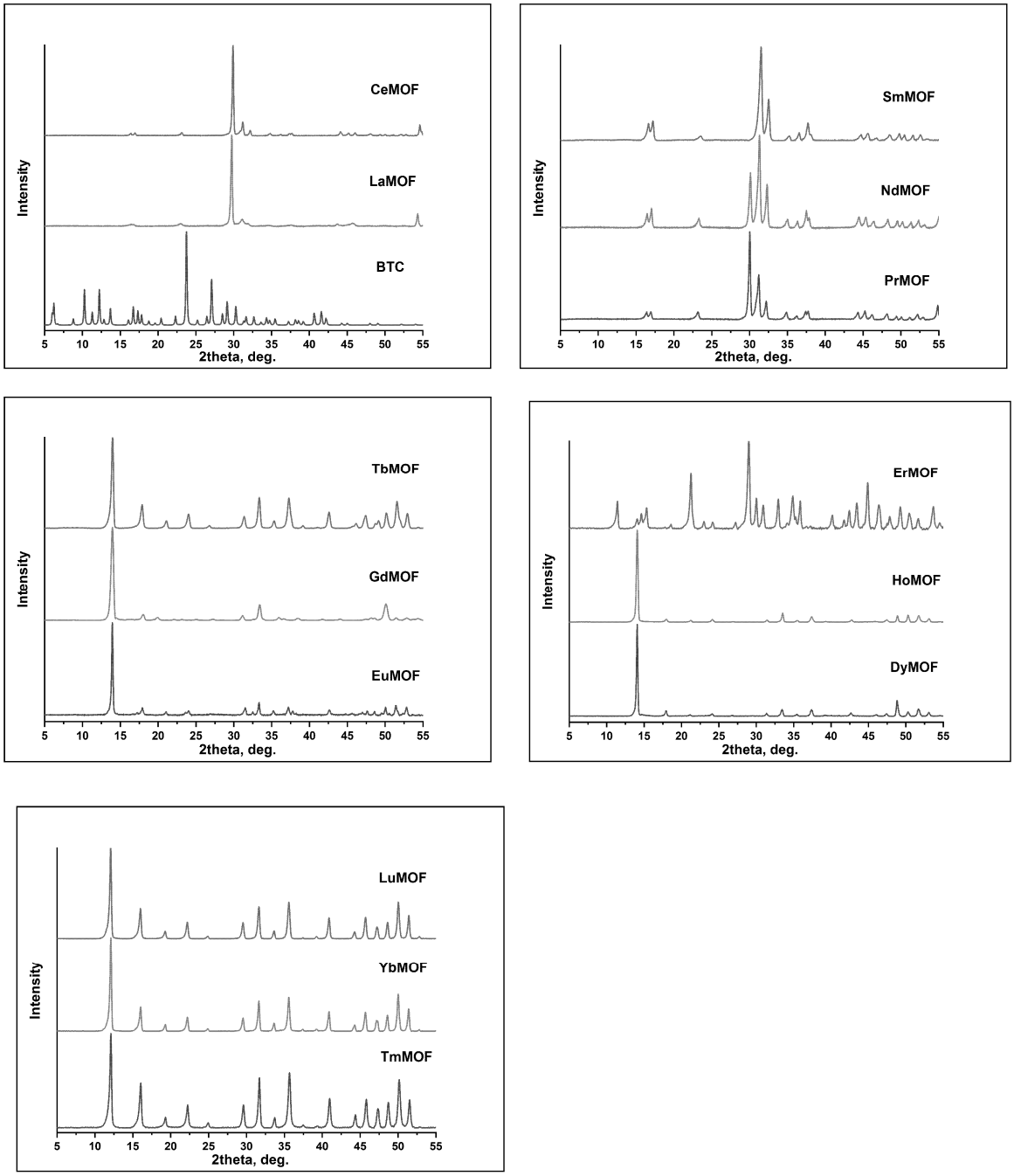

Figure 2. XRD patterns of synthesised lanthanide (Ln = La-Lu) metal-organic frameworks.

3.2. Infrared (FTIR) Spectroscopy

All the FTIR spectra of synthesized lanthanide metal-organic frameworks were very similar (see Figure 3). Asymmetric and symmetric stretching vibrations of the BTC ligand carboxylate groups displayed bands at 1556 and 1382 cm^{-1}. The bands at 1621, 3078, 689, and 780 cm^{-1} are assigned to the vibration of aromatic skeleton of the benzene ring [12]. The bands at 1678 and 2915 cm^{-1} are assigned to *v*CO and the asymmetric stretching vibration of the $–CH_3$ group of the *N*,*N*-dimethylformamide molecules [12,13]. The absence of FTIR bands at 2658, 2544 (OCOOH), and 1691 (CCOOH) cm^{-1} indicates that the BTC ligands were completely deprotonated after the reaction. The broad band at 3420 cm^{-1} is attributed to the hydrogen-bonded *v*OH groups from adsorbed (residual) water (Table 2).

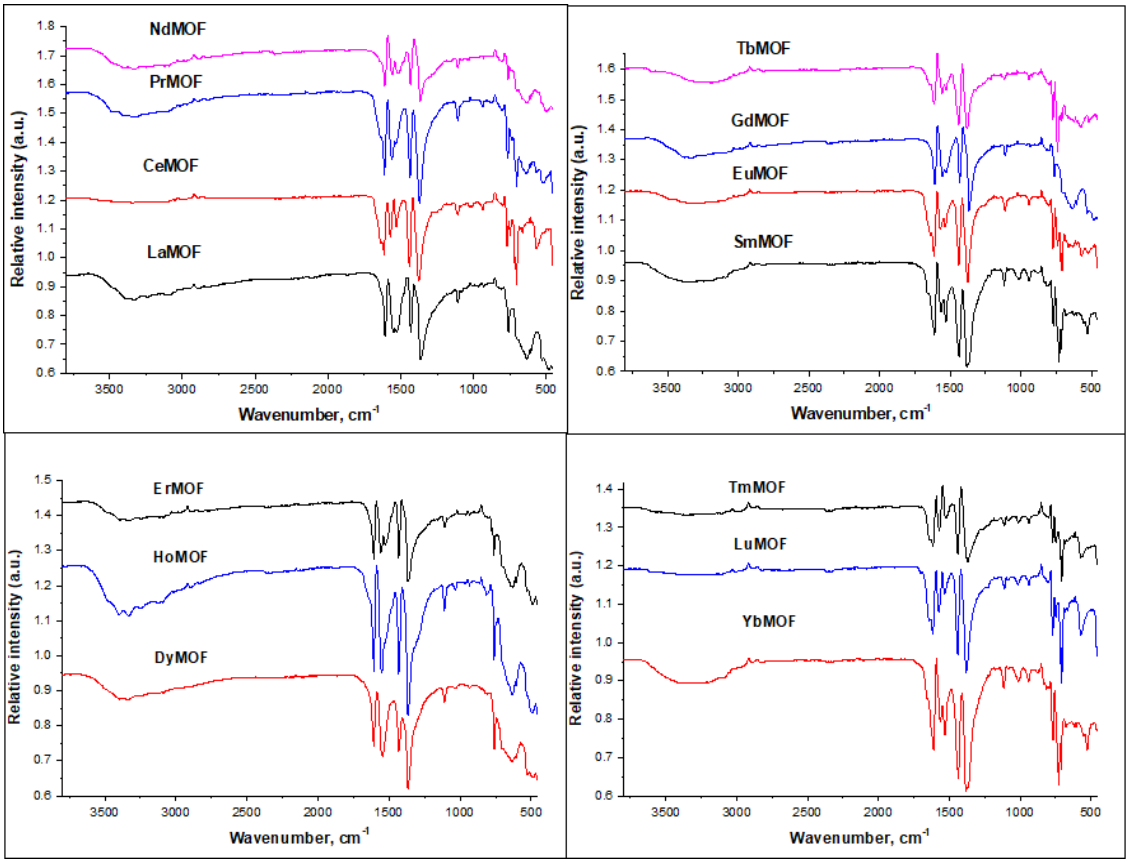

Figure 3. FTIR spectra of LnMOFs.

Table 2. FTIR assignments of synthesised LnMOFs.

Band Wavenumber, cm^{-1}	689 and 780	1382	1556	1678	2915	3420
Assignment	Vibrations of 1,4-substituted benzene ring	Sym. stretching of BTC carboxylic groups	Assym. stretching of BTC carboxylic groups	ν(=CO) of DMF	Assym. Stretch. of $-CH_3$ in DMF	ν(-OH) of absorbed, residual water

3.3. Thermal (TG/DTG) Analysis

The TG/DTG curves of synthesized lanthanide-containing MOFs are shown in Figure 4.

As seen, all the MOF samples had similar thermal stability [14,15]. The first mass loss in DTG curves was observed at about 120 °C (except for CeMOFs at ~200 °C). This first weight loss in the temperature range of 20–160 °C corresponds to the loss of water molecules and adsorbed moisture. The main mass loss, which continuously occurred up to 400–450 °C, is assigned to the decomposition of DMF. At higher temperatures (above 450 °C) the mass loss is associated with final decomposition of MOFs and formation of $Ln_2O_2CO_3$, or $Ln_2(CO_3)_3$ and Ln_2O_3 [16–18].

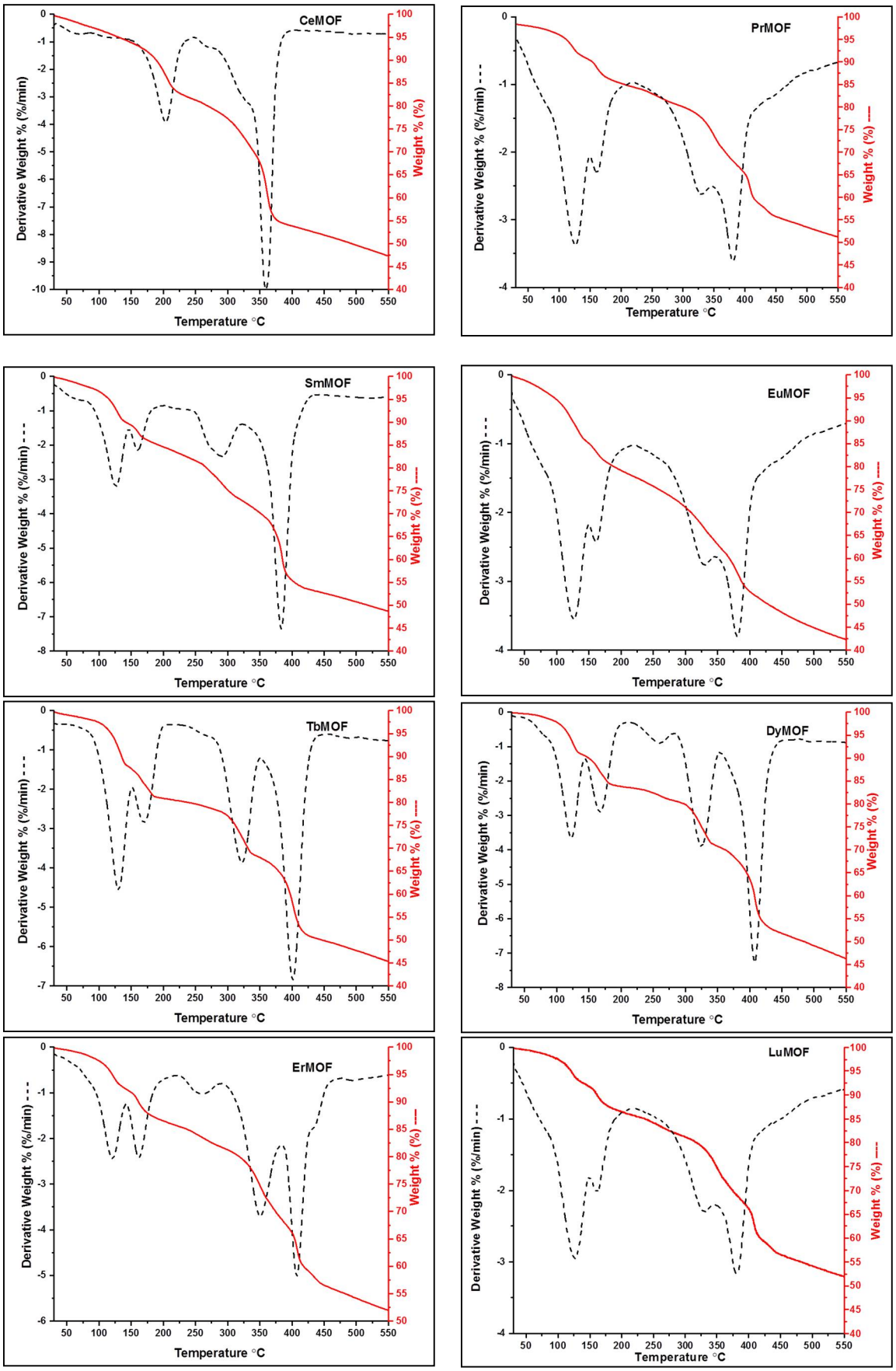

Figure 4. TG and DTG curves of synthesised lanthanide-containing MOFs.

3.4. Luminescent Properties

It is well-known that lanthanides, especially Eu and Tb, can absorb ultraviolet radiation efficiently through an allowed electronic transition to convert to excited state $^5D_4$, and these excited states are deactivated to the multiplet ^7F_J states by emitting visible light. Emission spectra of Pr, Sm, Eu, and Tb metal-organic frameworks are shown in Figure 5. The intensity of emission lines situated at 325, 416, and 443 nm (UV—blue region) of PrMOF (λ_{ex} = 290 nm) were very weak.

The emission lines for SmMOF (λ_{ex} = 275 nm) are assigned to $^4G_{5/2}\rightarrow{}^6H_{5/2}$, $^4G_{5/2}\rightarrow{}^6H_{7/2}$, $^4G_{5/2}\rightarrow{}^6H_{9/2}$, and $^4G_{5/2}\rightarrow{}^6H_{11/2}$ transitions at 563, 601, 649 and 702 nm (yellow—orange region). The emission lines of synthesized EuMOF (λ_{ex} = 285 nm) are assigned to $^5D_0\rightarrow{}^7F_0$, $^5D_0\rightarrow{}^7F_1$, $^5D_0\rightarrow{}^7F_2$, $^5D_0\rightarrow{}^7F_3$, and $^5D_0\rightarrow{}^7F_4$ transitions at 579, 593, 613, 618, and 699 nm, respectively (orange—red region). It can be observed that a very intense $^5D_0\rightarrow{}^7F_2$ transition at 613 nm in the emission spectrum was dominating. It is known that the $^5D_0\rightarrow{}^7F_2$ transition is an electric dipole transition and is very sensitive to the local symmetry of europium ions. For the TbMOF (λ_{ex} = 285 nm) the emission lines are assigned to $^5D_4\rightarrow{}^7F_6$, $^5D_4\rightarrow{}^7F_5$, $^5D_4\rightarrow{}^7F_4$, $^5D_4\rightarrow{}^7F_3$, $^5D_4\rightarrow{}^7F_2$, $^5D_4\rightarrow{}^7F_0$ transitions at 488, 542, 582, 620, 646, and 679 nm, respectively (blue green—green region). Very intense $^5D_4\rightarrow{}^7F_5$ transition at 542 nm is observed in the emission spectrum of TbMOF.

The photoluminescence measurements showed that Ce and La MOFs with BTC ligands are optically inactive. This is in a good agreement with the literature data [16,17]. The synthesized Nd, Gd, Dy, Ho, Er, Tm, Yb, Lu metal-organic frameworks, however, displayed very weak or even undetectable fluorescence at excitation wavelengths of 250–400 nm.

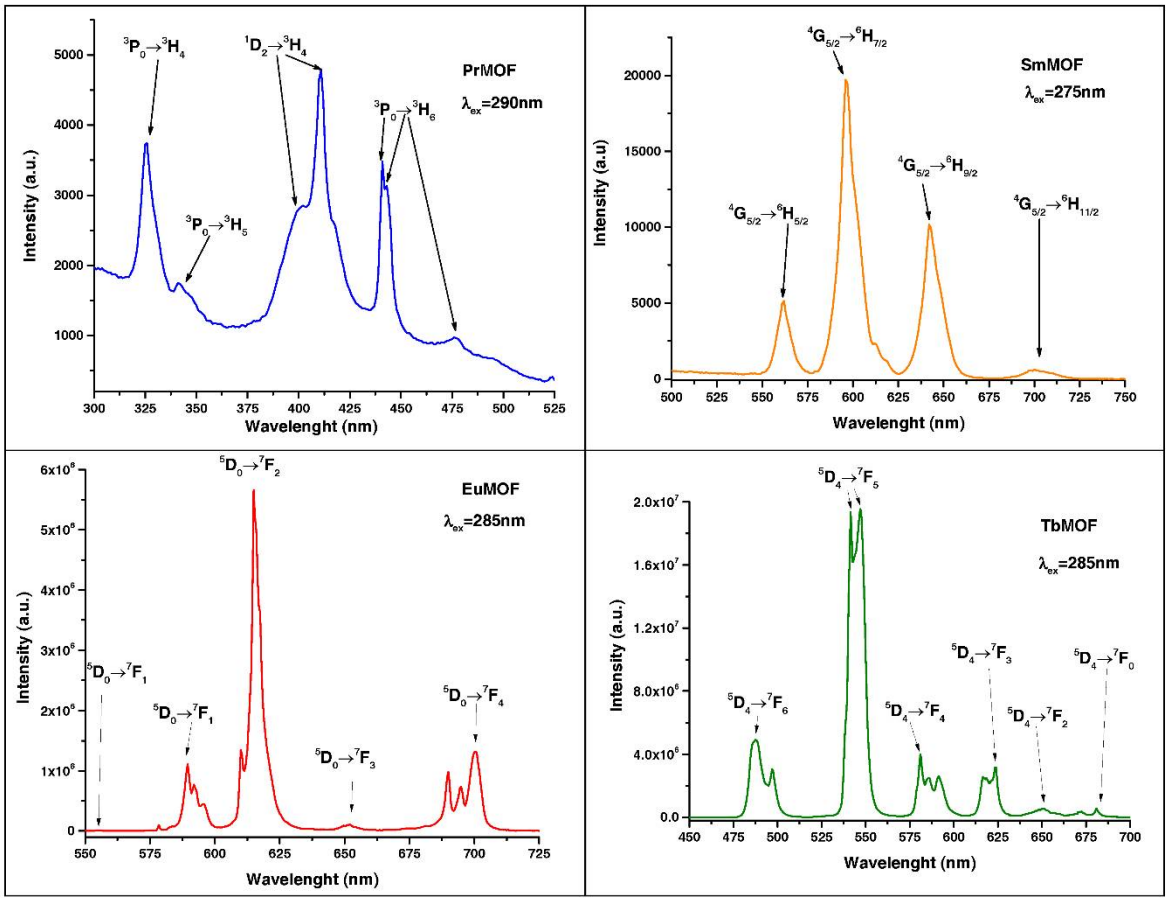

Figure 5. Emission spectra of Pr, Sm, Eu and Tb metal-organic frameworks.

3.5. Scanning Electron Microscopy

The representative SEM micrographs of synthesized lanthanide MOFs are shown in Figure 6.

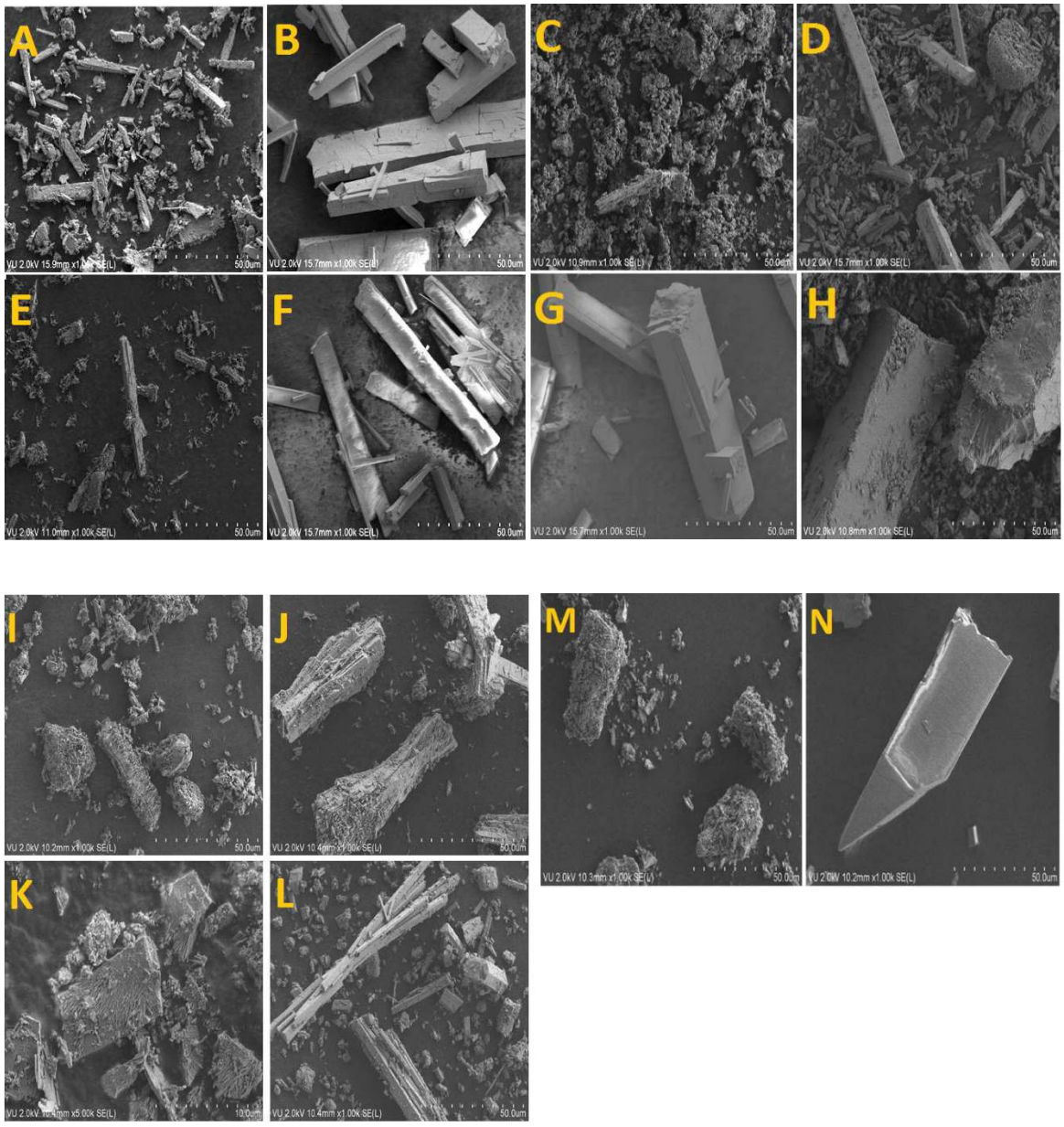

Figure 6. SEM images of synthesised metal-organic frameworks: Ce (**A**), Pr (**B**), Nd (**C**), Sm (**D**), Tb (**E**), Eu (**F**), Er (**G**), Ho (**H**), Tm (**I**), La (**J**), Gd (**K**), Dy (**L**), Yb (**M**), Lu (**N**).

The SEM results revealed that all compounds consist of two types of particles. In most of the cases the formed rectangular plate-like crystallites of 25–70 μm in size were covered with nanosized differently shaped particles. We can conclude that nature of lanthanide does not influence significantly the surface morphology of fabricated lanthanide MOFs.

4. Conclusions

The lanthanide metal-organic frameworks Ln(BTC)$(DMF)_2(H_2O)$ (LnMOFs) (Ln = La, Ce, Pr, Nd, Sm, Eu, Tb, Dy, Ho, Er, Tm, Yb and Lu) were successfully synthesized using 1,3,5-benzenetricarboxylic acid (BTC) as a coordination ligand. These MOFs were obtained with very well-developed crystalline

structure. All FTIR spectra of LnMOFs showed characteristic asymmetric and symmetric stretching vibration bands of the BTC ligand. The emission spectra of Pr, Sm, Eu, and Tb metal-organic frameworks were discussed in this study, however, the La, Ce, Nd, Gd, Dy, Ho, Er, Tm, Yb, and Lu metal-organic frameworks displayed very weak or even undetectable fluorescence at excitation wavelengths of 250–400 nm. The SEM micrographs of synthesized lanthanide MOFs showed the formation rectangular plate-like crystallites of 25–70 μm in size covered with nanosized differently shaped particles.

Author Contributions: Conceptualization, A.K. and A.L.; Methodology, A.B.; Software, A.L.; Validation, A.L., A.B. and A.K.; Formal Analysis, A.B.; Investigation, A.L.; Resources, A.K.; Data Curation, A.L., A.B. and A.K.; Writing-Original Draft Preparation, A.L.; Writing-Review & Editing, A.K.; Visualization, A.K.; Supervision, A.K.; Project Administration, A.B.; Funding Acquisition, A.K.

Funding: This research was funded by a grant SINALAN (No. S-LU-18-13) from the Research Council of Lithuania.

Conflicts of Interest: The authors declare no conflict of interest.

References

1. Guo, X.D.; Zhu, G.S.; Fang, Q.R.; Xue, M.; Tian, G.; Sun, J.Y.; Li, X.T.; Qiu, S.L. Synthesis, Structure and Luminescent Properties of Rare Earth Coordination Polymers Constructed from Paddle-Wheel Building Blocks. *Inorg. Chem.* **2005**, *44*, 3850–3855. [CrossRef] [PubMed]
2. Wang, L.H.; Li, P.F. Synthesis, Structure, and Catalytic Activity of A New Mn(II) Complex with 1,4-Phenylenediacetic Acid and 1,10-Phenanthroline. *Bull. Chem. React. Eng. Catal.* **2018**, *13*, 1–6. [CrossRef]
3. Rosi, N.L.; Kim, J.; Eddaoudi, M.; Chen, B.L.; O'Keeffe, M.; Yaghi, O.M. Rod Packings and Metal−Organic Frameworks Constructed from Rod-Shaped Secondary Building Units. *J. Am. Chem. Soc.* **2005**, *127*, 1504–1518. [CrossRef] [PubMed]
4. Laurikenas, A.; Katelnikovas, A.; Skaudzius, R.; Kareiva, A. Synthesis and characterization of Tb3+ and Eu^{3+} metal-organic frameworks with $TFBDC^{2-}$ linkers. *Opt. Mater.* **2018**, in press.
5. Li, Y.L.; Yu, C.; Yang, B.; Liu, Z.R.; Xia, P.Y.; Wang, Q. Target-catalyzed hairpin assembly and metal-organic frameworks mediated nonenzymatic co-reaction for multiple signal amplification detection of miR-122 in human serum. *Biosens. Bioelctron.* **2018**, *102*, 307–315. [CrossRef] [PubMed]
6. Li, X.Y.; Zhang, J.L.; Han, Y.; Zhu, M.Y.; Shang, S.S.; Li, W. MOF-derived various morphologies of N-doped carbon composites for acetylene hydrochlorination. *J. Mater. Sci.* **2018**, *53*, 4913–4926. [CrossRef]
7. Liu, X.M.; Tang, B.; Long, J.L.; Zhang, W.; Liu, X.H.; Mirza, Z. The development of MOFs-based nanomaterials in heterogeneous organocatalysis. *Sci. Bull.* **2018**, *63*, 502–524. [CrossRef]
8. Valizadeh, B.; Nguyen, T.N.; Stylianou, K.C. Shape engineering of metal-organic frameworks. *Polyhedron* **2018**, *145*, 1–15. [CrossRef]
9. Stackhouse, C.A.; Ma, S.Q. Azamacrocyclic-based metal organic frameworks: Design strategies and applications. *Polyhedron* **2018**, *145*, 154–165. [CrossRef]
10. Echaide-Gorriz, C.; Clement, C.; Cacho-Bailo, F.; Tellez, C.; Coronas, J. New strategies based on microfluidics for the synthesis of metal-organic frameworks and their membranes. *J. Mater. Chem. A* **2018**, *6*, 5485–5506. [CrossRef]
11. Van Vleet, M.J.; Weng, T.T.; Li, X.Y.; Schmidt, J.R. In Situ, Time-Resolved, and Mechanistic Studies of Metal-Organic Framework Nucleation and Growth. *Chem. Rev.* **2018**, *118*, 3681–3721. [CrossRef] [PubMed]
12. Furukawa, H.; Cordova, K.E.; O'Keeffe, M.; Yaghi, O.M. The Chemistry and Applications of Metal-Organic Frameworks. *Science* **2013**, *341*. [CrossRef] [PubMed]
13. Wu, Y.; Qiu, L.-G.; Wang, W.; Li, Z.-Q.; Xu, T.; Wu, Z.-Y.; Jiang, X. Kinetics of oxidation of hydroquinone to p-benzoquinone catalyzed by microporous metal-organic frameworks $M_3(BTC)_2$ [M = copper(II), cobalt(II), or nickel(II); BTC = benzene-1,3,5-tricarboxylate] using molecular oxygen. *Transit. Met. Chem.* **2009**, *34*, 263–268. [CrossRef]
14. Faustini, M.; Kim, J.; Jeong, G.-Y.; Kim, J.Y. Microfluidic Approach toward Continuous and Ultrafast Synthesis of Metal–Organic Framework Crystals and Hetero Structures in Confined Microdroplets. *J. Am. Chem. Soc.* **2013**, *135*, 14619–14626. [CrossRef] [PubMed]

15. Almáši, M.; Zeleňák, V.; Opanasenko, M.; Císařová, I. Ce(III) and Lu(III) metal–organic frameworks with Lewis acid metal sites: Preparation, sorption properties and catalytic activity in Knoevenagel condensation. *Catal. Today* **2015**, *243*, 184–194. [CrossRef]
16. Peng, M.M.; Jeon, U.J.; Ganesh, M.; Aziz, A.; Vinodh, R.; Palanichamy, M.; Jang, H.T. Oxidation of Ethylbenzene Using Nickel Oxide Supported Metal Organic Framework Catalyst. *Bull. Korean Chem. Soc.* **2014**, *35*, 3213–3218. [CrossRef]
17. Da Luz, L.L.; Viana, B.F.; Oliveira da Silva, G.; Gatto, C.C.; Fontes, A.M. Controlling the energy transfer in lanthanide–organic frameworks for the production of white-light emitting materials. *CrystEngCom* **2014**, *16*, 6914–6918. [CrossRef]
18. Kareiva, A.; Karppinen, M.; Niinistö, L. Sol-gel synthesis of superconducting $YBa_2Cu_4O_8$ using acetate and tartrate precursors. *J. Mater. Chem.* **1994**, *4*, 1267–1270. [CrossRef]